Vietnam Journal of Earth Sciences, 45(4), 531-552, https://doi.org/10.15625/2615-9783/19026

Vietnam Journal of Earth Sciences
https://vjs.ac.vn/index.php/jse

Benthic habitat mapping and assessment of seagrass species diversity in Da Lon Reef, Truong Sa Islands, Vietnam, using very high-resolution satellite imagery and in situ data

Hoi Dang Nguyen[1], Dung Trung Ngo[1*], Dung Viet Vu[2]

[1]*Institute of Tropical Ecology, Joint Vietnam-Russia Tropical Science and Technology Research Center, Cau Giay District, Hanoi, Vietnam*
[2]*Coast Branch - Joint Vietnam-Russia Tropical Science and Technology Research Center, Nha Trang City, Khanh Hoa, Vietnam*

Received 02 March 2023; Received in revised form 27 July 2023; Accepted 26 September 2023

ABSTRACT

Benthic habitats are critical in shallow sea areas; they regulate the diversity and richness of organisms in each area. Mapping benthic habitats elucidates natural sea characteristics and aids in managing and using natural resources, as well as conserving marine biodiversity. This study established a benthic habitat map for the Da Lon Reef area, Truong Sa Islands, Vietnam, using Pléiades high-resolution remote sensing imaging materials and field survey results from 2020 and 2021. We identified seven classes of benthic habitats with a 91.64% overall accuracy, corresponding to a Kappa coefficient of 0.88. In the Da Lon Reef, seagrass biomes occupy a large area (more than 200 ha) and are distributed mainly inside lagoons at depths of 2–6 m. The field survey results identified five seagrass species and the biodiversity and biomass of seagrass populations in the lagoon of Da Lon Reef. The study results confirm the fundamental value of resources, biodiversity in general and seagrass in particular, in managing and protecting shallow sea ecosystems and biodiversity conservation in the Da Lon Reef area, an important part of the Truong Sa Islands, Vietnam.

Keywords: Benthic habitat mapping, Pleiades, seagrass, Dalon Reef, Truong Sa islands.

1. Introduction

Benthic habitats house several marine species, including prominent biomes such as corals, seagrass, seaweed, and reef fish, and constitute bottom materials/sediments such as sand, mud, and dead corals (Anggoro et al., 2015; Butler et al., 2021). For example, in the Da Lon Reef (Discovery Great Reef), Truong Sa Islands, Vietnam, coral reefs, seagrass beds, reef fish, abdominal groups, cephalopods, and bottom material primarily comprising coral sandy sediments are predominant in the shallow sea zone. However, studies on biodiversity and spatial distribution databases of marine biomes at Da Lon Reef are limited by objective factors such as the offshore island sea and the complexity of field investigations and surveys. This hinders the determination of the distribution of bottom biomes, thus adversely affecting the management of resources and the conservation of regional ecosystems. These limitations necessitate mapping and constructing a spatial database related to the habitat of the bottom biomes on the offshore island for biodiversity

*Corresponding author, Email: ngotrungdung266@gmail.com

conservation (Harris et al., 2012). Benthic habitat maps have four distinct advantages: (1) aiding the government in planning, managing, and making decisions on marine space; (2) supporting and underpinning the design of marine protected areas; (3) contributing to scientific research programs aimed at elucidating bottom ecosystems and seafloor geology; and (4) providing reference for assessments of living and non-living seabed resources for economic and managerial purposes, including the design of fishing reserves (Harris et al., 2012).

Satellite imagery is an effective tool for establishing geospatial databases. Maps established from satellite imagery provide more effective and accurate information than maps established solely from descriptive methods and field observations (Nababan et al., 2021). Remote sensing and GIS methods have been extensively employed for shallow sea habitat mapping in numerous regions worldwide (Kendall et al., 2017; Porskamp et al., 2018; Smith et al., 2019; Wicaksono, 2014; Wicaksono, Fauzan, et al., 2019). Numerous remote sensing images have been used to map benthic habitats in shallow water zones, yielding varying results (Dekker, Mount et al., 2007). The Airborne Visible/Infrared Imaging Spectrometer imaging application and Lens-Induced Granulomatous Uveitis algorithms, CIUB, with wavelengths of 400–675 nm in Kaneohe Bay, Hawaii, have distinguished benthic habitats, including coral, sand, and algae (Velez-Reyes et al., 2006). In Qatar's coastal zone and Halul Island, the WorldView-2 photo app distinguishes 10 types of benthic habitats using Environment for Visualizing Images (ENVI) and eCognition software (Butler et al., 2020). The overall accuracy of error assessment using ENVI was 80%, with a Kappa coefficient of 0.71 for data processing using ENVI software. The overall accuracy of error assessment using eCognition is 94%, with a Kappa coefficient of 0.92 for data processing using eCognition software. Using Landsat 8-OLI multispectral satellite images, we mapped benthic ecosystems in the Red Sea, including 22 different habitat classifications (Khaled et al., 2020). The overall accuracy of the benthic habitat assessment was 66.7%, with an overall Kappa coefficient value of 0.611. The Worldview-2 image was used to map the bottom habitat classification in Bangsring, Banyuwangi Regency, resulting in relatively high accuracy: 71.23% at Level 1 and 59.62% at Level 2 (Sinaga et al., 2016). Sentinel-2 MSI remote sensing imaging has also been used to establish benthic habitat maps near the shore of Derawan Island with up to 75% accuracy (Fauzan, 2016). The satellite imaging app PlanetScope categorizes the habitats of bottom organisms, including coral reefs, seagrass, macroalgae, and bottom habitats (Al Hadi et al., 2021). Moreover, Landsat remote sensing imagery has been used in studies of the Great Barrier Reef to classify 15 reef cover classes (Kennedy et al., 2021). Numerous medium- and low-resolution satellite images have been used to map benthic habitats in different seas with 60–75% accuracy. The Pléiades image is a very high-resolution satellite image (Taha et al., 2021), with a resolution of 0.5 m for all four bands (blue, green, red, and near-infrared), capable of establishing a highly accurate benthic habitat map. The resolution of the Pléiades satellite imagery is superior to that of other types of satellite images, such as Sentinel-2 (10 m × 10 m for four bands of blue, green, red, and near-infrared images) (Fernandez et al., 2013) and Landsat-8 OLI (15 m × 15 m for panchromatic) (Roy et al., 2014).

Based on satellite imaging materials, numerous methods have been used to classify seabed environments in shallow sea zones. In particular, pixel- and object-based methods using maximum likelihood (ML) have been employed. For the Padaido Islands, Papua, Indonesia, Hafizt (Hafizt et al., 2017) used

Landsat-8 OLI satellite imagery to compare the abovementioned methods. Both methods output benthic habitat maps with seven classes. The pixel-based classification improved overall accuracy (47.57%) in mapping benthic habitats compared with the object-based classification approach (36.17%). In the Kemujan Island study using Quickbird satellite imagery, the overall accuracy levels of pixel-based image classification and the ML method were 64.28% and 73.30%, respectively (Wicaksono et al., 2017).

Additionally, using an object-based classification based on Sentinel-2 images in Labuan Bajo waters, East Nusa Tenggara, Indonesia, a map for the classification of the bottom organism environment was formed with an overall accuracy of >80%. Based on the above studies, object-based classification of images has more advantages and is more accurate than pixel-based classification of images. Unlike classifying objects based only on single pixels, the algorithm for object classification is based on the continuous spatial properties of pixels, such as structure and spatial relationships. Usually, these generated batches do not have an attribute value. The state name needed according to the classification system has not been determined (Navulur, 2006). Benthic habitat mapping has been used in numerous studies, such as in the Polish Exclusive Zone of the Southern Baltic (Janowski et al., 2021) and Indonesia (Wahidin et al., 2015).

Using high-resolution satellite imagery and object classification methods on the recognition software is highly effective concerning the overall accuracy index and Kappa coefficient. Therefore, using high-resolution remote sensing images and object classification methods to construct benthic habitat maps is necessary. According to our survey in 2020 and 2021, seagrass is one of the characteristic ecosystems in the Da Lon Reef area and is widely distributed in the lagoon area. Seagrass biomes are habitats for numerous marine species, such as Echinoidea, Gastropoda, Coleoidea, and reef fish (Ruiz Fernandez et al., 2009). Seagrass also plays a role in stabilizing sediments and protecting the coast from erosion (Mellors et al., 2002). Seagrass is one of the most critically endangered ecosystems globally, but little is known about it because it is often submerged and not easily visible (Short et al., 2016). Globally, seagrass habitats are endangered by numerous anthropological factors (Grech et al., 2012). Therefore, assessing the distribution and biodiversity of this critical type of marine ecosystem forms the basis for the management and conservation of managers.

The main objectives of this study are 1. to map the bottom biotopes of Da Lon Reef using high-resolution satellite imagery and seafloor measurement data and 2. to assess the diversity of species composition and biomass of seagrass beds using data from specimens obtained from field surveys. This elucidation forms the basis for conserving and restoring seagrass bed ecosystems in the Da Lon Reef area, Spratly Islands.

2. Materials and Methods

2.1. Study area

Da Lon Reef is an atoll reef in the Nam Yet island cluster, Truong Sa Islands, Vietnam, 286 nautical miles east of Khanh Hoa Province. This coral reef is located in the north-south direction and spans a length of 15.2 km and a width of 1.7 km (Hancox et al., 1995). The coral shelf of the island is closed; inside the beach, there is one lake, which is approximately 10 km long and 1 km wide. During high tide throughout the floodplain, numerous orphan rocks rise out of the water when the tide drops to 0.5 m on the beach.

Da Lon Reef, which is affected by solar radiation, belongs to the Truong Sa Islands region. The East Asian monsoon regime is the northeast monsoon, which occurs from

November to April, and the southwest monsoon occurs from June to September. The highest average air temperature was observed in April (29.5°C), and the lowest was observed in January (26.6°C). The highest average rainfall occurred in November (341 mm), and the lowest occurred in March (62 mm) (Mau et al., 2020). The wave mode in the region depends on the monsoon: the prevailing wave direction is northeast with an average elevation of 2.5 m and shifts to the southwest with an average elevation of 1.65 m for the northeast and southwest monsoons. The subsurface current around the coral bedrock was approximately 10–30 cm/s. The area has an asymmetric heliometric regime, with a high water level of 1.8–2.2 m and a low water level of 0–0.1 m (Dang et al., 2022).

2.2. Remote sensing data

In this study, we used Pléiades remote sensing imaging obtained on October 21, 2020, to establish a benthic habitat map in Da Lon Reef, Truong Sa Islands, Vietnam (Fig. 1). Multispectral and panchromatic products were acquired using the KCB-TS03 project. Multispectral imagery at a 1.5 m spatial resolution consisted of four bands: blue (430–545 nm), green (466–620 nm), red (590–710 nm), and near-infrared (715–918 nm). The panchromatic image comprised a single band (405–1053 nm) at a 0.5 spatial resolution. The raw multispectral and panchromatic images were combined using the pansharp module (Barrell et al., 2015) of ArcGIS 10.8 software to create a multispectral image with a spatial resolution of 0.5 m.

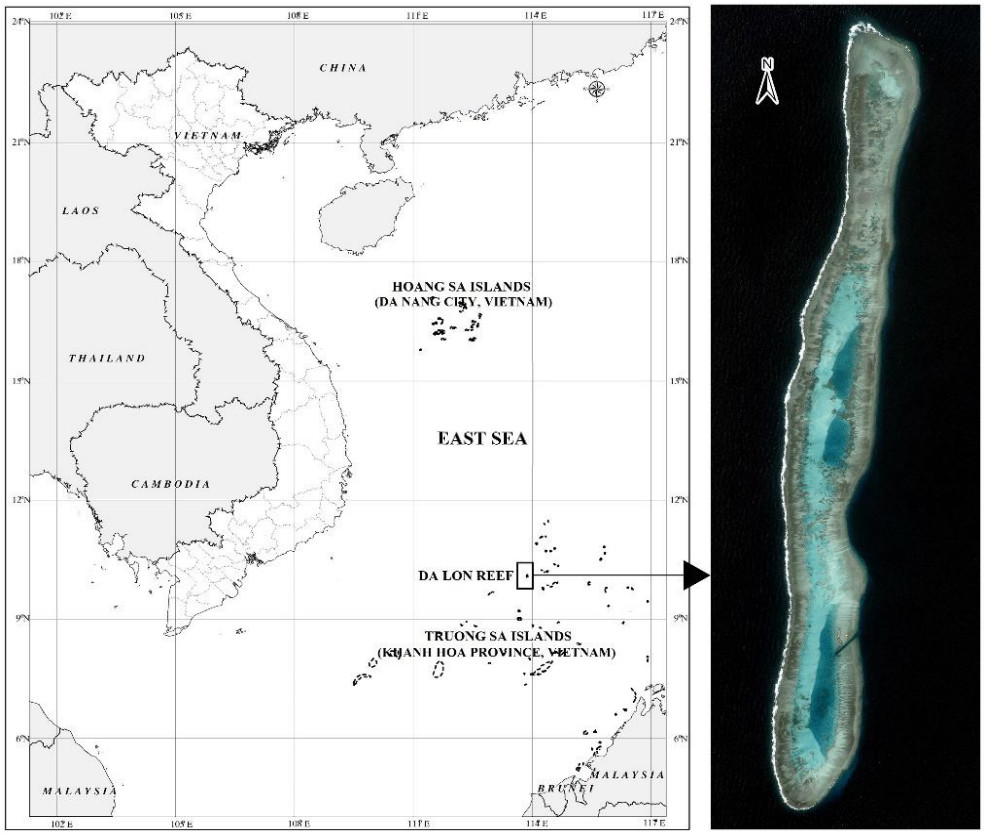

Figure 1. Location of Da Lon Reef and Pléiades remote sensing imagery in the Da Lon Reef area, resolution 0.5 m × 0.5 m

2.3. In-situ measurement data

2.3.1. Collection of spatial patterns and verification of images

The collection of samples for the classification, testing, and identification of such biomes at Da Lon Reef was conducted through field trips (October and November 2020). Accordingly, we collected samples of classified images based on the scuba diving method at depths of 2–6 m and snorkeling. A pair of waterproof Gopro Hero 7 with built-in GPS and a Canon G7x MkIII with waterproof housing was used to capture still photos and footage videos along the survey lines and surrounding areas in each diving session. Nevertheless, images of the dual Gopros and Canon compact cameras were set at 12 MP and 20 MP, respectively, with an auto white balance and shutter speed to optimize the ground truth data capture. Footage videos were recorded using dual GoPro cameras along transects at a resolution of 2.7 k and frame rate of 30 fps to compensate for light reduction due to water column absorption and cloudy conditions. Nevertheless, photos and footage videos were recorded vertically to avoid distortion, particularly at the edge of the frame. The data, samples, photos, videos, and measurements from the field survey (Fig. 5) form the basis for a detailed description of the typical benthic habitats of the Da Lon Reef. The uncrewed aerial vehicle (UAV) images (Figs. 5m, n, o, and p) after flight were shaped to the standard coordinate system compared to the Pléiades image and used for comparison with the micrograms and sample points of the remote sensing image. This comparison enhances the accuracy of the image interpretation sample points. Accordingly, a total of 3,020 field sample points were taken, of which 80% of the samples (2,416 samples) were used for the image interpretation process, and the remaining 20% of the samples (604 samples) were used to evaluate the accuracy of the map.

2.3.2. Collection and evaluation of seagrass biome biodiversity

Samples were collected from research island points via scuba diving, cameras, and underwater video recording. Coverage was determined using a dosing frame of 100 cm × 100 cm (Fig. 2) divided into 100 10 cm × 10 cm cells (Short, F. et al., 2002).

At each survey point, three 50 m long cross sections (symbols A, B, and C) were placed in the east-west direction (Kirkman, 1996). The intersection 25 m from each cross-section was marked. The cells determined the coverage set at points 0, 5, 10, 15, 20, 25, 30, 35, 40, 45, and 50 m (11 cells for 1 transect) (Supplementary Material) (Fig. 3).

Figure 2. Survey and measurement of seagrass cover

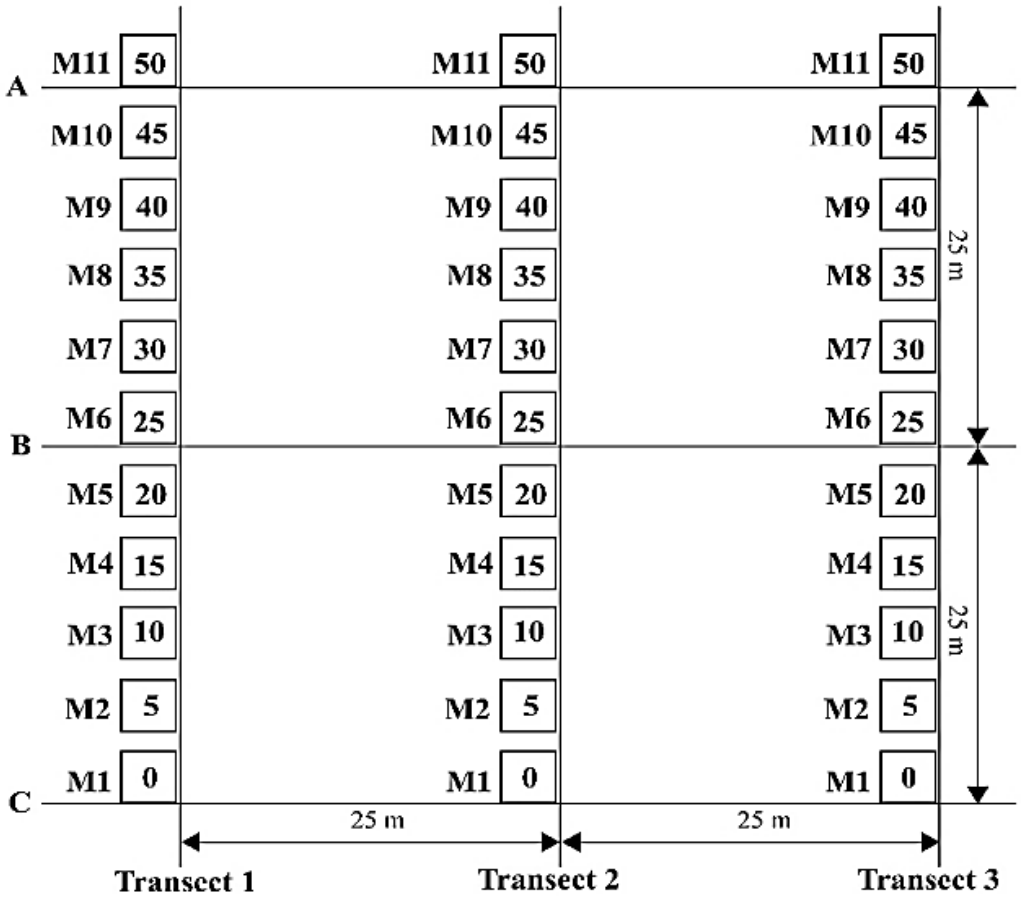

Figure 3. Seagrass study cross-sectional diagram

The species composition was determined at the sampling site, and the coverage was determined according to 11 quantitative frames of each cross-section at the research site. At each cross-section, four samples (three quantitative and one qualitative sample) were collected at three locations 25 m apart (Short, F. et al., 2002).

2.4. Methods

2.4.1. Image segmentation and benthic habitat mapping

GBNDVI calculation

A layer of vegetation index was calculated and stacked into the satellite image to enhance the segmentation and classification results. The results of classification studies of remote sensing images show that the blue and green bands are sensitive to objects in the marine environment (Hafeez et al., 2018; Mascarenhas et al., 2018). Therefore, we use the green-blue normalized difference vegetation index to map the seagrass distribution in the Nam Yet island area using the following formula (Dang Hoi et al., 2022):

$$GBNDVI = \frac{Nir - (Green + Blue)}{Nir + (Green + Blue)} \quad (1)$$

Fig. 4a shows the green-blue NDVI map of Da Lon Reef calculated from the Pléiades satellite imagery and the locations of the 604 training samples (Fig. 4b).

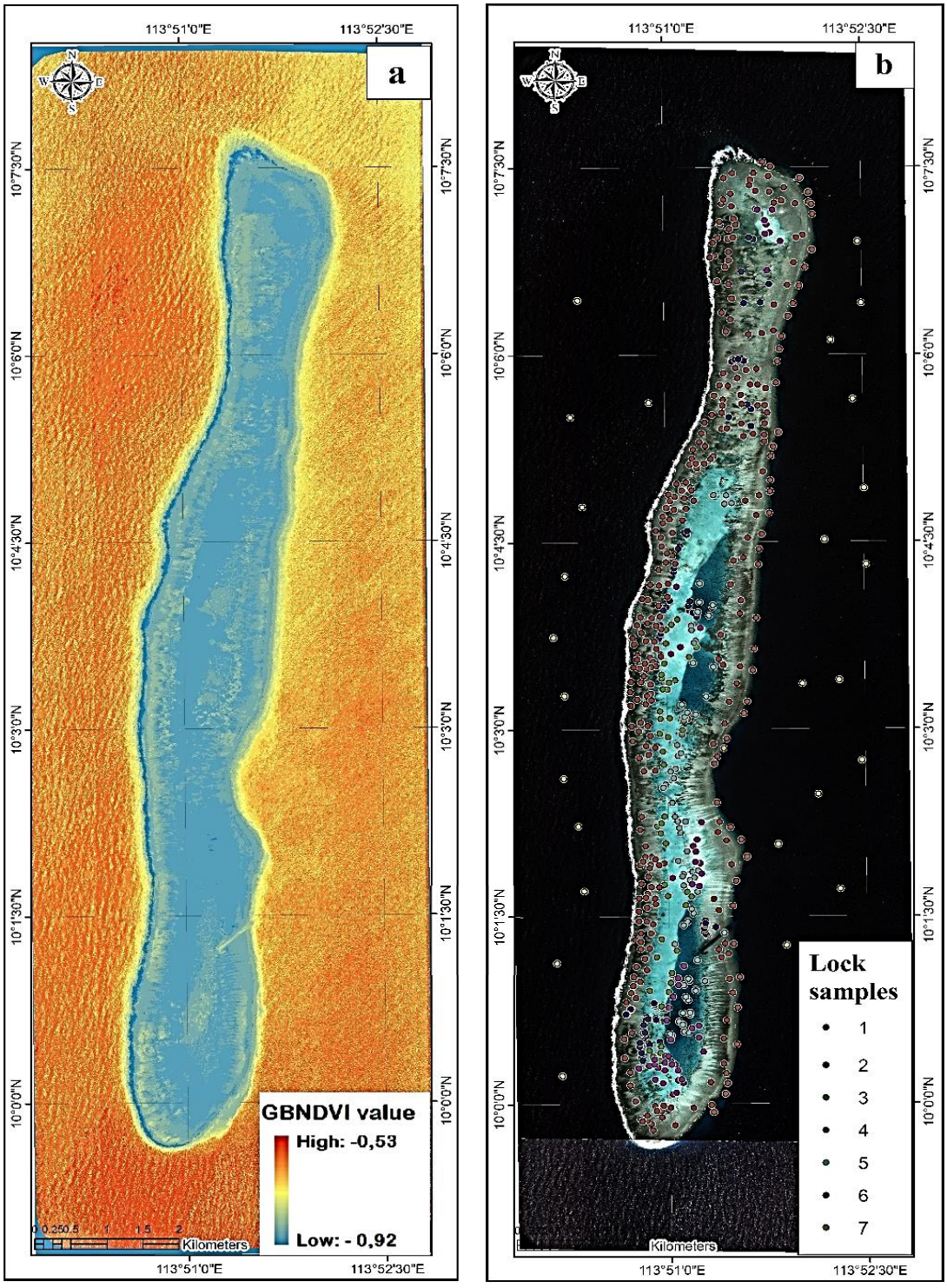

Figure 4. a) Green-blue NDVI map of the Da Lon Reef area on October 21, 2020;
b) 604 lock samples in the Da Lon Reef area

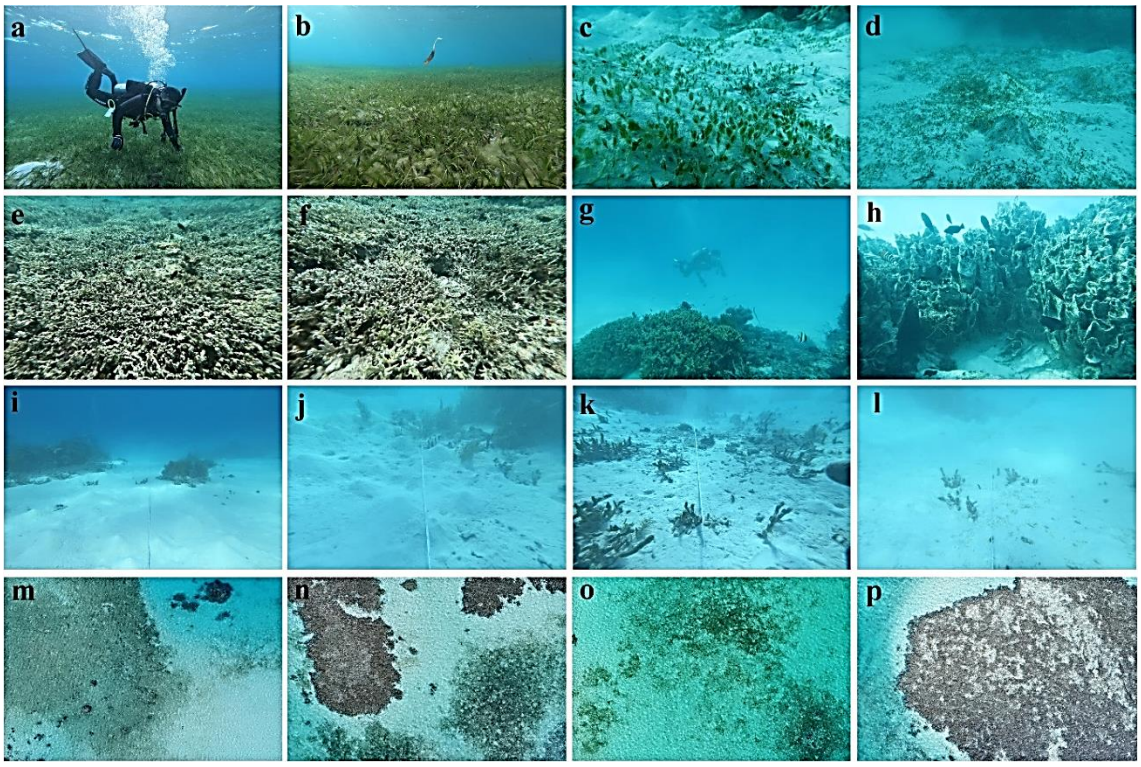

Figure 5. Field survey photos of Da Lon Reef for classification and verification of map accuracy (a, b, c, d: seagrass biome; e, f, g, h: coral biome; i, j, k, l: sandy sediment and coral debris; and m, n, o, p: seagrass, coral, and sandy sediment biomes via UAV photo)

Image segmentation and habitat classification

The Pléiades satellite picture was used to identify 604 categorization training samples from 7 benthic habitats in the Da Lon Reef region: construction (36 samples); seagrass (56 samples) (Figs. 5a, b, c, d, and o); seagrass and sandy sediment (50 samples); coral reef (310 samples) (Fig. 5e, f, g, h); block coral in the lagoon (69 samples) (Fig. 5m, n, p); sandy sediment and coral debris (54 samples) (Fig. 5i, j, k, l); and deep-sea surface (n = 29).

Subsequently, recognition software was utilized using the object-oriented classification technique to categorize and elucidate pictures based on critical patterns of image decoding. Benthic habitats were recorded and categorized based on picture tone, structure, form, and connection with adjoining areas. This approach is a form of supervised classification based on the notion of reflectance differences between coated objects using the following process (Fig. 6):

Verification of classification results

Based on 604 classification sample points and field survey results, the accuracy of the classification results for benthic habitat maps was assessed. A confusion matrix was built between the classification result, Kappa (K) test, and evaluation sample. According to Congalton (1999), matrix tables are the most effective methods for assessing accuracy (Congalton et al., 1999): overall accuracy (OA), user's Accuracy (UA), and producer's accuracy (PA).

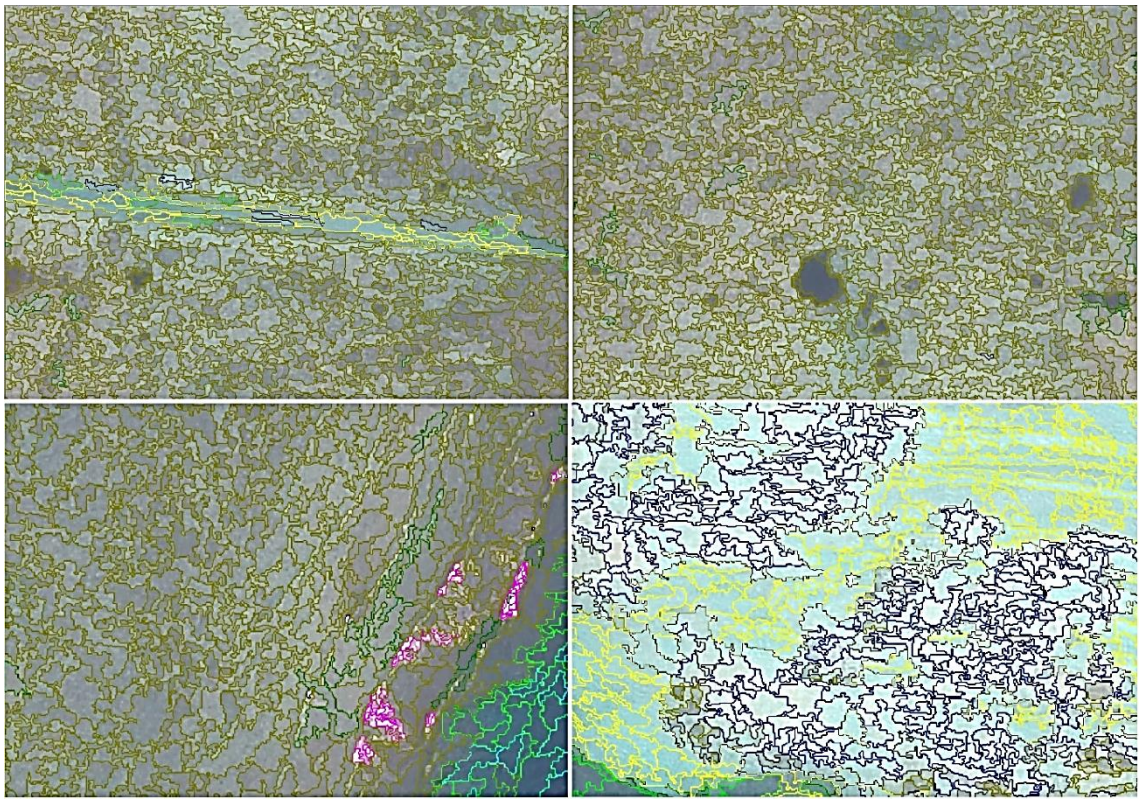

Figure 6. Segment objects of specific images in eCognition software

The Kappa coefficient was used as a measure of classification accuracy. This is the utility coefficient of all elements from the error matrix and is the fundamental difference between what is real about the deviation error of the matrix and the total number of changes indicated by the rows and columns (McGrath, 2010). The Kappa value was expressed as follows:

$$K = \frac{N\sum_{i=1}^{r} X_{ii} - \sum_{i=1}^{r}(X_{i+} - X_{+i})}{N^2 - \sum_{i=1}^{r}(X_{i+} - X_{+i})} \quad (1)$$

where r is the number of columns in the image matrix, X_{ii} is the number of pixels observed in row i and column i (on the main diagonal), Xi_{+} is the total number of pixels observed in row i, X is the total number of pixels observed in column i, and N is the total number of pixels observed in the image matrix.

The Kappa coefficient usually ranges between 0 and 1, and the classification accuracy is acceptable. According to the U.S. Geological Survey, Kappa has three value groups: $K \geq 0.8$: high accuracy; $0.4 \leq K < 0.8$: moderate accuracy; and $K < 0.4$: low accuracy.

2.4.2. Seagrass species diversity, coverage, and biomass

The C (%) coverage of seagrass was determined according to the formula (Short, F. T. et al., 2002):

$$C = \frac{\sum(Mi\ x\ fi)}{\sum f} \quad (2)$$

where Mi is the mid-point of class i and fi is the frequency comprising cells with the same class number i.

The seagrass cover level, as described by English et al. (1997), is presented in Table 1 (English et al., 1997). Seagrass areas with less than 10% coverage are not measured by transect but only use a quantitative framework to calculate the average seagrass cover for the entire area.

Table 1. Assessment of seagrass cover by English et al. (1977)

Class	Amount of substratum covered	% Substratum covered	Midpoint %
5	1/2 to all	50–100	75
4	1/4 to 1/2	25–50	37.5
3	1/8 to 1/4	12,5–25	18.75
2	1/16 to 1/8	6,25–12,5	9.38
1	less than 1/16	< 6,25	3.13
0	absent	0	0

After collection, the seagrass samples were fixed in the DESS solution (Table 2) (Yoder et al., 2006). In the laboratory, treated seagrass samples are classified based on a seagrass classification system that constitutes morphological criteria, such as flowers, fruits, seeds, leaf tendons, tannin cells, serrated teeth at the leaf edge, and leaf tops (Hartog, 1970; Phillips et al., 1988).

Table 2. DESS solution (250 mL) for fixing seagrass samples

Disodium EDTA FW 374,24	23,265 g
1 M NaOH	To pH EDTA to 8.0
Dimethyl Sulfoxide (DMSO)	50 mL
NaCl	Enough to saturate the solution
Deionized water	Enough to bring the final volume up to 250 ml

3. Results

3.1. Benthic habitat map of Da Lon Reef

3.1.1. Accuracy assessment of image classification

Based on the examination results of 604 image analysis samples and formulas for calculating the Kappa coefficient (K; Formula 1), the overall accuracy matrix table for the benthic habitat map of the Da Lon Reef area in 2020 (Table 3) was established.

Table 3. Confusion matrix and accuracy assessment of benthic habitat classification in the Da Lon Reef area

		Ground Reference							Total
		Construction	Seagrass	Seagrass and sandy sediment	Coral reef	Block coral in the lagoon	Sandy sediment and coral debris	Deep sea surface	
Classification	Construction	**35**	0	0	0	1	0	0	**36**
	Seagrass	0	**50**	2	2	1	1	0	**56**
	Seagrass and sandy sediment	0	1	**46**	1	0	2	0	**50**
	Coral reef	0	9	3	**290**	4	4	0	**310**
	Block coral in the lagoon	0	1	1	1	**63**	2	1	**69**
	Sandy sediment and coral debris	1	0	2	1	1	**49**	0	**54**
	Deep sea surface	0	0	0	0	0	1	**28**	**29**
Total		**36**	**61**	**54**	**295**	**70**	**59**	**29**	**604**
User Accuracy (%)		97,22	81,97	85,19	98,31	90,00	83,05	96,55	**90,33**
Producer Accuracy (%)		97,22	89,29	92,00	93,55	91,30	90,74	96,55	**92,95**
Overall accuracy (%)									**91,64**

Table 3 shows that the overall accuracy index is 91.64%, corresponding to K = 0.91. Accordingly, groups of subjects prone to misinterpretation include coral reefs and seagrass (accounting for 3% of both sample types), coral reefs and block coral in lagoons (accounting for 1.32% of both sample types), and coral reef and sandy sediment and coral debris (accounting for 1.37% of both sample types). The rest of the groups had a small number of misinterpreted patterns.

According to Table 3, the construction and seagrass subjects yielded high user accuracy values (97–98%), while the seagrass group yielded the lowest (81.97%). The seagrass, sandy sediment, and sandy sediment and coral debris groups yielded higher user accuracy values than the other groups (85.19 and

83.05%, respectively). The construction group yielded the highest user accuracy value (97.22%), followed by the deep-sea surface group. Other groups of subjects exhibited relatively high producer accuracy values, ranging from 89% to 93%.

Based on the Pléiades satellite image classification, a benthic habitat map consisting of seven different benthic habitat classes was established for the Da Lon Reef area (Fig. 7): construction (2.02 ha); seagrass (67.58 ha); seagrass and sandy sediment (113.90 ha); coral reef (1.419.99 ha); block coral in lagoon (50.42 ha); sandy sediment and coral debris (459.86 ha); and deep-sea surface.

According to Fig. 7, three constructions form living structures on the reef floor, distributed at the north and south ends of the Da Lon Reef. The coral reefs are distributed around the Da Lon Reef, forming continuous reef surfaces with an average depth of 0.5–1 m at low tide. This is the most significant type of benthic habitat, accounting for 67% of the total area of the 6 types of benthic habitats (except the deep-sea surface). High-density seagrass beds are scattered inside the lagoon of the Da Lon Reef, often adjacent to the inner reaches of coral reefs. Similarly, the seagrass and sandy sediment distribution spaces are located in the lagoon of Da Lon Reff, adjacent to coral reefs and high-density seagrass areas. The coral reefs are concentrated in the south and east of the Da Lon Reef. According to the field survey results, the reef in the Da Lon Reef area can be divided into three main areas: (a) Reef surface: with a depth of 0.5–2 m at the receding tide, mainly hard reef-forming corals such as *Porites cylindrica*, *Pocillopora verrucosa*, and *Pachyseris rugosa*; (b) Inner reef area: mostly *Acropora formosa* coral biomes at a 2 m depth; (c) Outer reef area: Extending over the surface of the reef down to a 40 m depth are the dominant Acropora corals such as *Acropora hyacinthus*, *Acropora spicifera,* and *Acropora anthoceris*. In addition, numerous soft corals include *Lobophytum crebriplicatum, Sinularia abrupta,* and *Sinularia leptolados*. From a depth of approximately ≤40 m, Gorgonaria corals growing on areas with slopes ranging from 70° to 85° in steepness are predominant. In addition, sandy sediment and coral debris are concentrated in the lagoon, north and central Da Lon Reef. This type of benthic habitat has a depth of 2–6 m. Coral masses in this lagoon include numerous reef-forming corals of the genera Acropora and Montipora interspersed with soft corals.

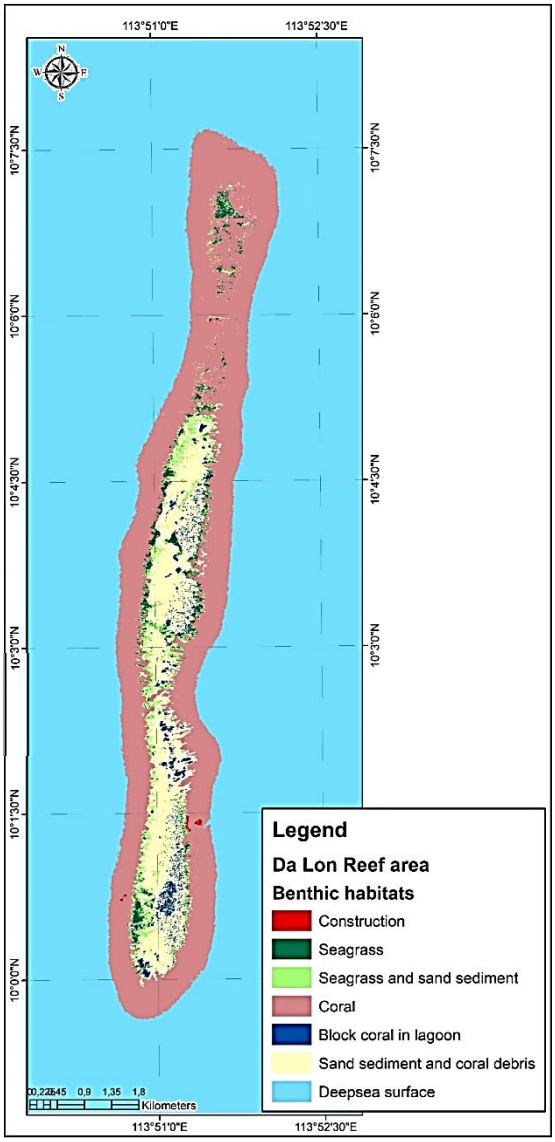

Figure 7. Benthic habitat map of the Da Lon Reef area

Spectral reflectance coefficients of specific benthic habitats

As shown in Fig. 8a, differences were observed between the spectral reflectivity of benthic habitats. Overall, these groups of subjects had the highest spectral reflectivity values for the blue bands, with reflectance values of 1609, 873, 1081, 781, 1266, and 1421 for subjects 1 to 6, respectively. The second-highest spectrum reflectivity values belonged to the green, red, and NIR bands. However, the values for each benthic habitat group differed.

For the construction group, which is the only group of subjects with a surface on the water, the spectral reflection for the photo bands was relatively strong, which differed from the remaining groups of subjects below the water surface (Fig. 8a). The spectral reflectivity values for spectral bands of seagrass and coral reef subjects were relatively close to each other. However, the spectral reflectivity value of the seagrass group was more stable and had a higher average value than that of the coral reef. These two subject groups exhibited the highest rate of confusion in the image interpretation process in the Da Lon Reef area. The reflected spectrum value of spectral bands for the seagrass and sandy sediment subjects was higher than that for the seagrass and coral reef subjects, which exhibited a spectrum value stability in the red band (Fig. 8a). The spectrum reflectivity value for all four coral bands in the lagoon block group was higher than that for the three bands of the seagrass, seagrass and sandy sediment, and coral reef groups. However, the spectral reflectivity value for all four bands (ranging from 350 to 850 for the red band, 550 to 1250 for the green band, 850 to 1500 for the green band with the blue band, and 250 to 480 for the NIR band) was not highly stable. For sandy sediment and coral debris subjects, the spectral reflex values of the three bands (red, green, and blue) exceeded those of the other groups of underwater subjects. Nevertheless, the spectral reflectivity value of the NIR band (250 to 300) was similar to that of seagrass and sandy sediment subjects (Fig. 8a).

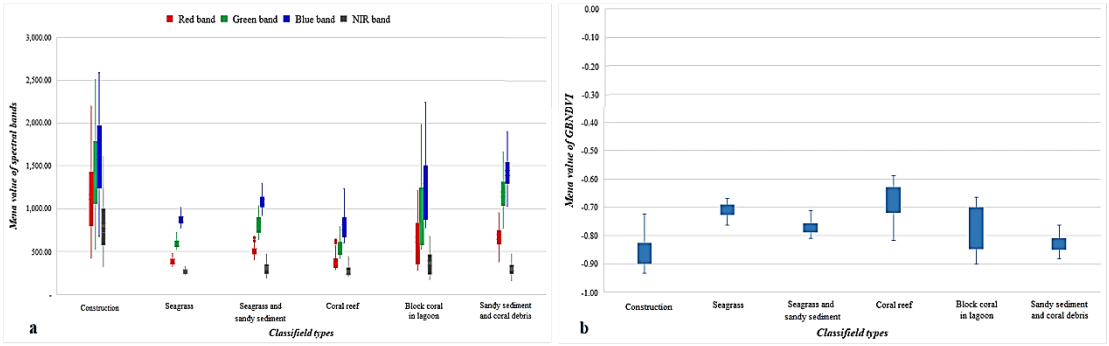

Figure 8. Comparison of the mean values and standard deviation of spectral reflectance by classified types of benthic habitats: a) the four bands (red band, green band, blue band, and NIR band); b) GBNDVI

The GBNDVI value of the subject groups was relatively low, ranging from -0.90 to -0.63 (Fig. 8b). In particular, the GBNDVI value of the coral group was the highest, ranging from -0.72 to -0.63. In contrast, the seagrass, seagrass and sandy sediment, and

sandy sediment and coral debris groups had relatively stable GBNDVI values compared to the rest of the target groups, with levels ranging from 0.2 to 0.3.

3.1.2. Distribution of benthic habitats

In the Da Lon Reef area, the characteristic ecosystems include corals, seagrass, and other forms of sandy sediment (Fig. 7). In particular, coral ecosystems are divided into two types: (1) coral reefs and (2) block corals in the lagoon. The outer section of the reef has a significant slope, especially east of the Da Lon Reef, with an average slope of 75–85°. The coral ecosystem here is diverse, with numerous common coral species, including *Pocillopora verrucosa, Montipora stellata, Isopora brueggemanni*, and *Porites lobata*. In the western region, which has relatively low-gradient terrain slopes (50–75°), the coral species composition is highly diverse, with the advantages of *Porites rus, P. lutea, P. nigrescens, Pocillopora verrucosa, Pocillopora eydouxi, Goniastrea pectinata,* and *Pocillopora woodjonesi.* Both regions have diverse reef fish biomes dominated by *Chaetodon auripes, Cirrhitus pinnulatus, Acanthurus* spp., *Thalassoma hardwicke, Oxycheilinus unifasciatus, Cheilinus* spp., *Labroides dimidiatus,* and *Halichoeres hortulanus.* The reef surface has a flat terrain; the dominant reef species are Acropora and Porites. Fish diversity was not high, mainly for species of the families Grammistidae, Lutjanidae, and Pomacentridae. There are numerous mass corals with a single distribution and low diversity in the lagoon of Da Lon Reef, with individuals belonging to the family Faviidae and the species *Montipora digitata* and *M. cactus* of the family Acroporidae.

Seagrass biomes dominate the lagoon area of Da Lon Reef, covering 181.48 ha, where the area of the seagrass population has extensive coverage, forming continuous seagrass beds (67.58 ha). Consequently, numerous benthic species of Echinoidea, Gastropoda, Coleoidea, and other reef fishes have been recorded in areas with high-density seagrass beds. However, for areas with low seagrass densities, mainly the dominant *Halophila ovalis* species, only Gastropoda and Bivalvia species were recorded, and the density was low. In contrast, that of the seagrass areas was high.

3.2. Seagrass species diversity and biomass

3.2.1. Seagrass species diversity

The sample collection and analysis results revealed that the Da Lon Reef marine community included two species, as shown in Table 4. In addition, five seagrass species were collected and classified in the Da Lon Reef area. In particular, the seagrass species *Thalassia hemprichii* and *Syringodium isoetifolium* are predominant with a high density, thus forming continuous seagrass beds, which are habitable for numerous bottom species, typically Gastropod and Coleoidea species.

Seagrass species were uneven in different areas of the Da Lon Reef lagoon (Table 4). At a 2 m depth in the DaLon-1 area north of Da Lon Reef, the highest level of diversity was recorded for three species of seagrass: *Thalassia hemprichii, Halodule uninervis,* and *Cymodocea rotundata.* At a 2 m depth in the DaLon-2 area in the central area, the appearance of two seagrass species, *Syringodium isoetifolium* and *Halophila ovalis,* was recorded. Similarly, two seagrass species, *Thalassia hemprichii* and *Halodule uninervis,* were observed at a 2 m depth in the

DaLon-3 region. The lowest diversity level was in the DaLon-4 area south of the Da Lon Reef, which has a depth of approximately 6 m, recording only one species of *Halophila ovalis* seagrass with low density, scattered on the background of sandy sediments.

Table 4. Composition of seagrass species in the Da Lon Reef

No	Da Lon	Coordinate	Deep (m)	Coverage (%)	Species
1	DaLon-1	10° 0'29.63"N 113°51'5.08"E	2 m	51,18 ± 6,48	*Thalassia hemprichii* *Halodule uninervis* *Cymodocea rotundata*
2	DaLon-2	10° 1'35.51"N 113°51'9.32"E	2 m	10,34 ± 1,93	*Syringodium isoetifolium* *Halophila ovalis*
3	DaLon-3	10° 3'14.98"N 113°51'1.42"E	2 m	< 5%	*Thalassia hemprichii* *Halodule uninervis*
4	DaLon-4	10° 4'0.16"N 113°51'14.99"E	6 m	< 5%	*Halophila ovalis*

3.2.2. Seagrass morphology

Based on the number of seagrass samples collected in the Da Lon Reef area, sampling and morphological descriptions of five species of seagrasses were obtained (Table 5 and Figs. 9 and 10).

Table 5. Morphological description of five seagrass species in the Da Lon Reef area

№	Species	Morphology		
		Leaf	**Stem**	**Rhizome**
1	*Syringodium isoetifolium* (Fig. 8a)	Cylindrical leaf structure Leaf sheath length: 1-3.5 cm	Stems erect at each node, bearing 2 leaves.	Smooth 1–3 small, branched roots
2	*Thalassia hemprichii* (Fig. 8b)	Length: 6–12.5 cm Width: 0.3–0.7 cm. Curved and rounded at the tips of the leaves.	Short, straight bearing 2–6 leaves.	Thick Covered with triangular leaf scars
3	*Halodule uninervis* (Fig. 8c)	Length: up to 12 cm, Width: 0.2–0.5 cm, Linear and flat. The margins are smooth, and the tips of the leaves have three distinct tips, one in the middle and one on the sides.	Short, growing upright at each node Number of leaves per stem: 2–3 leaves.	Smooth
4	*Halophila ovalis* (Fig. 8d)	Length: 1.38 cm, width 1.05 cm Shape: oval. Sheathless, with two scales covering the base of the petiole. **Microscopic leaf anatomy:** 15 cross veins in each leaf Transvenous branching is rare. Distance between veins: 0.7 mm, diagonal angle: 65°. Leaf margins are smooth, and the leaf surface is hairless.	Petiole length: 1.7–2.1 cm Grows directly from rhizomes. Pairs of leaves on petioles.	Smooth, thin, and light in color.
5	*Cymodocea rotundata* (Fig. 9)	Length: 5–22 cm, 0.4–0.6 cm wide, Shape: Straight and flat, 2 rounded leaf tips The leaf sheath is 3–6 cm long. There are 13 longitudinal veins.	Short, straight at each node Number of leaves per stem: 3 leaves.	Smooth, At each node, there are two irregularly branched roots.

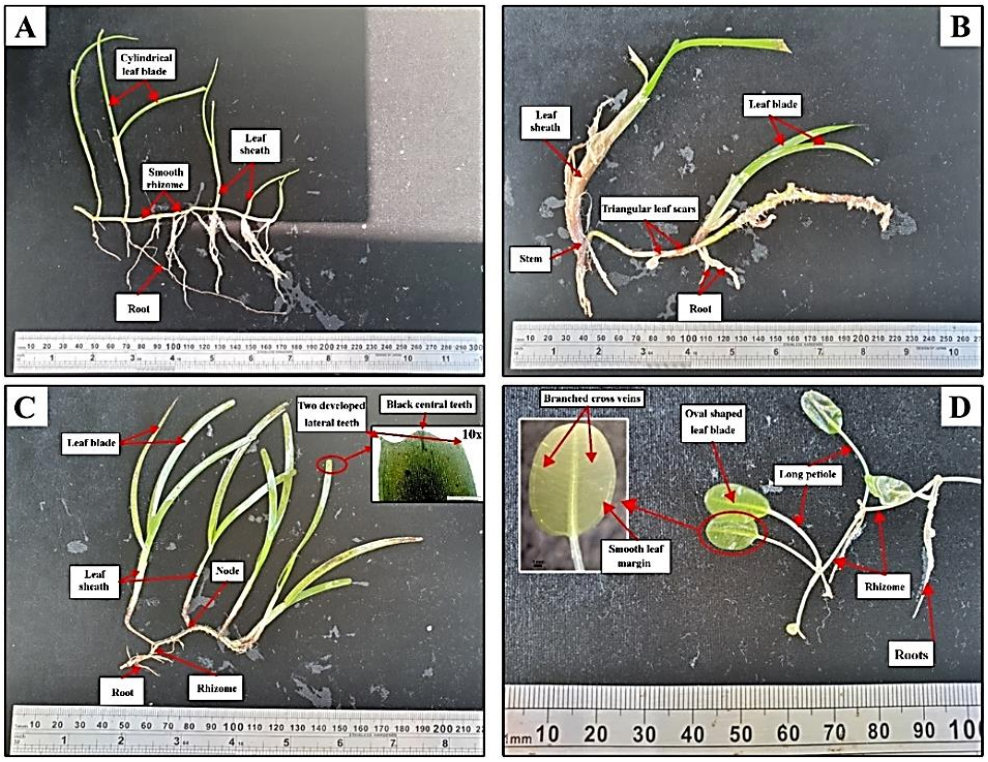

Figure 9. Morphology of seagrass in the Da Lon Reef: a) *Syringodium isoetifolium*; b) *Thalassia hemprichii*; c) *Halodule uninervis*; and d) *Halophila ovalis*

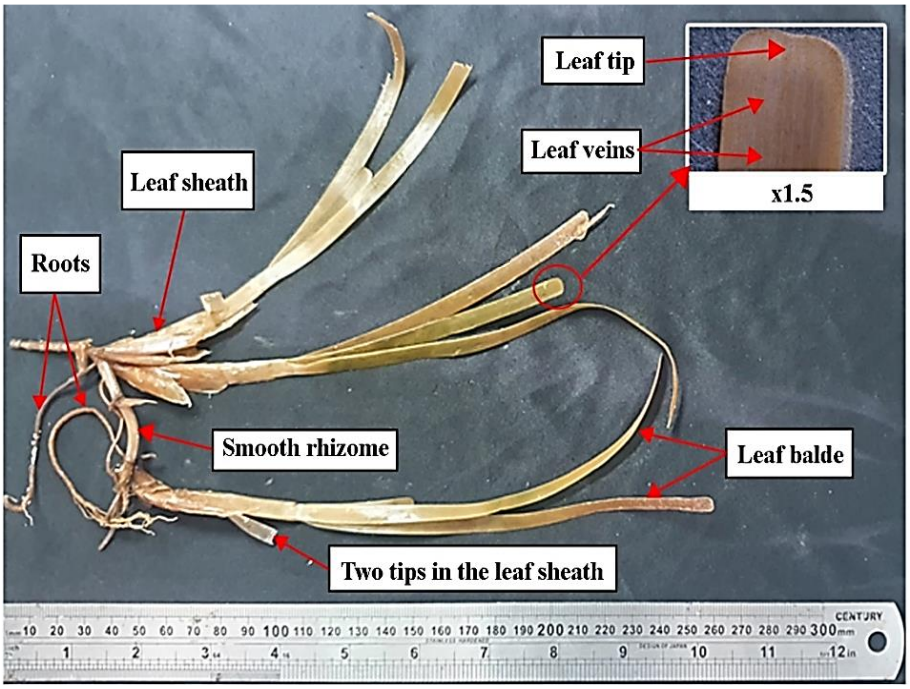

Figure 10. Morphology of *Cymodocea rotundata* in the Da Lon Reef

3.2.3. Seagrass coverage and biomass

According to the field survey results in the Da Lon Reef, seagrass populations grow in sandy sediment mixed with loose coral debris. In the Da Lon Reef area, seagrass cross-section measurements were performed to determine coverage in two areas of DaLon-1, where the seagrass is relatively thick, and DaLon-2, where seagrass grows relatively sparsely. In the DaLon-1 region, 3 species of seagrass, *Thalassia hemprichii, Halodule uninervis*, and *Cymodocea rotundata,* have been recorded. In the DaLon-2 area, two species of seagrasses, *Syringodium isoetifolium* and *Halophila ovalis,* have been recorded.

Accordingly, the DaLon-1 area has a seagrass coverage of class 5, the largest in the classification scale reported by English et al. (1977) (the average area is 51%) (Fig. 11). However, the stability of seagrass cover in DaLon-1 was not high, with a mean standard deviation of up to 6.48. In particular, in the DaLon-2 area, the coverage of seagrasses was considerably lower than that in the DaLon-1 area, reaching only class 2 according to the classification scale reported by English et al. (1977), with an average coverage value of only 10% (Fig. 11). However, the standard deviation value of this area was relatively low, averaging only 1.93, with high stability.

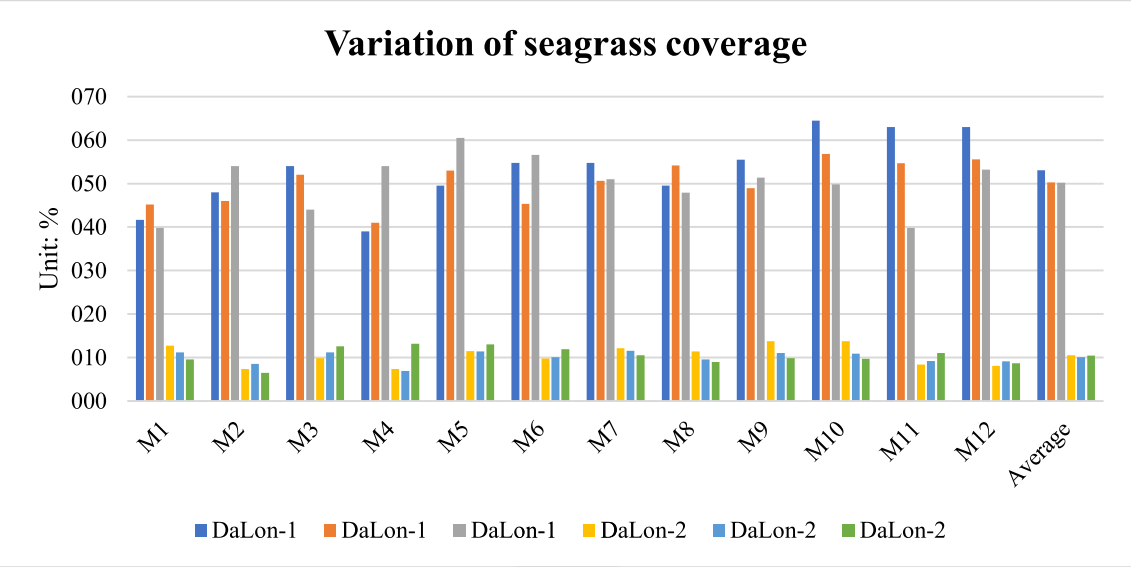

Figure 11. Fluctuations in coverage (%) of seagrass at transects in Da Lon Reef

The biomass of the five seagrass species recorded at Da Lon Reef was determined (Table 6). Specifically, *T. hemprichii* seagrass had the highest shoot density, reaching 1870 ± 235.65 shoot/m^2. The second-ranked was the seagrass *Syringodium isoetifolium,* with 560 ± 34.32 shoot/m^2. The remaining three seagrass species are valuable in low shoot density, ranging from 100 to 200 shoot/m^2, the lowest of which is *Cymodocea rotundata,* with a value of only 103 ± 9.54 shoot/m^2.

At the sample collection points, the biomass of *Thalassia hemprichii* seagrass also exhibited the highest value in both shoots and roots (149.6 ± 15.67 g/m^2 and 234.1 ± 9.24 g/m^2, respectively) (Table 6). *Halodule uninervis* ranked second, with a biomass value of 31.55 ± 5.33 g/m^2 for shoots and 18.46 ± 2.65 g/m^2 for roots. The lowest biomass out of the five seagrass species was exhibited by *Halophila ovalis,* with a value of 0.48 ± 0.0039 g/m^2 for shoots and 0.72 ±

0.00348 g/m^2 for roots. Biomass differences between seagrass species indicated strong and dominant growth of *Thallasia hemprichii* in the study area.

Table 6. Biomass of seagrass (shoot/m^2) in Da Lon Reef

№	Species	Density (shoot/m^2)	Dry biomass (DW)(g)	
			Shoot	Root
1	*Thalassia hemprichii*	1870 ± 235,65	149,6 ± 15,67	234,1 ± 9,24
2	*Syringodium isoetifolium*	560 ± 34,32	22,4 ± 4,53	16,8 ± 5,32
3	*Halodule uninervis*	210 ± 18,41	31,55 ± 5,33	18,46 ± 2,65
4	*Halophila ovalis*	120 ± 7,93	0,48 ± 0,0039	0,72 ± 0,00348
5	*Cymodocea rotundata*	103 ± 9,54	14,97 ± 2,297	8,78 ± 0,529

4. Discussions

The application of high-resolution remote sensing allows for the elucidation of spatial distribution and the establishment of spatial maps of benthic habitats in shallow seas. Concurrently, field surveys and verification improve map accuracy, specimen collection, and assessment of the biodiversity of bottom biomes, including seagrass biomes. In this study, we successfully mapped a coastal bottom habitat, including seagrass biomes, for the Da Lon Reef area of the Truong Sa Islands, Vietnam, based on high-resolution remote sensing imagery obtained from Pléiades using eCognition software. High-resolution remote sensing images are a suitable tool for determining the spatial range and distribution boundaries of benthic habitats and the spatial distribution of seagrass biomes in shallow zones (Dekker, Brando, et al., 2007; Ginting et al., 2021). Field surveys are essential for assessing the accuracy of bottom habitat maps. Simultaneously, this is an important research step for sample collection and assessment of the diversity and structure of seagrass communities. The mapping of the distribution of the bottom organism environment at Da Lon Reef yielded an overall accuracy of 90.02% and a Kappa coefficient of 0.89. Compared to the standards of the U.S. Geological Survey, the accuracy of the benthic habitat map in the Da Lon Reef area was highly accurate (K≥0.8). High-resolution Pléiades images allow for high-precision benthic habitat mapping, comparable to high-resolution image types such as Worldview-2 (OA = 88.3%) (Tamondong et al., 2013), and yield greater accuracy than medium-resolution photo types such as IKONOS (OA = 80%) (Tran Van, 2008), Quickbird satellite images (OA = 73.30%) (Wicaksono et al., 2017), and ALOS AVNIR-2 (OA = 78%) (Wicaksono, Fauzan, et al., 2019).

However, classification based on remote-sensing images for areas with low seagrass density is complex. Therefore, to supplement the database for taxonomic sampling, in addition to diving to survey the seabed, we used additional UAV data captured with a low-flight ceiling (10 m above the surface of the water) to supplement certain areas with low seagrass density. UAV imaging makes locating low-density seagrass distribution areas more accessible and accurate than simply surveying the area and comparing it to Pléiades remote sensing image.

This study identified the distribution of five seagrass species at Da Lon Reef, *Thalassia hemprichii, Syringodium isoetifolium, Halodule uninervis*, *Halophila ovalis,* and *Cymodocea rotundata*, and analyzed the structure of seagrass communities at different locations throughout the study area. The study results are comparable with our research on numerous other areas of the Truong Sa Islands. Accordingly, seagrass communities in Da Lon Reef have the highest diversity compared with other islands in the Truong Sa Islands (according to our field survey results in 2020

and 2021). However, compared to the Red Sea (12 species), Bintan (9 species), Florida Bay (7 species), and Brunei Darussalam (6 species), Da Lon Reef has a low diversity of seagrass (El Shaffai et al., 2011; Fourqurean et al., 2001; Khairunnisa et al., 2021; Lamit et al., 2017). In addition, certain seagrass distribution areas at Da Lon Reef have a relatively low density and small coverage when compared to certain islands in the Truong Sa Islands, such as Nam Yet Island (up to 82% south of the island) (Nguyen et al., 2022), Phan Vinh Island, and Son Ca Island (coverage of 70–80%, according to the survey results of our research team). The bottom of the seagrass populations on Da Lon Reef is still mostly sandy sediments and dead coral debris, similar to the seagrass biomes discovered in the Truong Sa Islands (Luong et al., 2020).

Based on the Da Lon Reef study results, in addition to mapping the distribution of the bottom organism-environment, remote sensing images can be used to map the biodiversity indicators of the bottom habitat, such as the Shannon index and Simpson and Shannon's Equitability index, as observed by Alberotanza et al. (Alberotanza et al., 2003), classify and describe the structure of seagrass biomes (Wicaksono et al., 2020), or determine the Leaf Area Index (LAI) value of seagrass (Hedley et al., 2016). In addition, unmanned aerial vehicles (UAVs) with multispectral cameras are suitable for shallow-, small-, and medium-sized scale mapping of the bottom organism-environment. This was also reported by Kabiri et al. (Kabiri et al., 2020). In addition to high-resolution satellite imagery, medium-resolution satellite imagery such as Quickbird and GeoEye-1 (Hassan et al., 2020) with OA = 91,2% can be used to enhance the accuracy of benthic habitat mapping. Different models and algorithms, such as the random forest classification algorithm (Wicaksono, Aryaguna et al., 2019), can also be applied to optimize the image classification process. These methods can be applied in subsequent studies.

Therefore, the application of high-resolution remote sensing integrated with surveys for describing, verifying, and collecting field samples (including the use of UAVs) is an appropriate method for mapping the distribution of the bottom organism environment in the shallow zones of coastal areas. The field study achieved quantification and visual description of bottom habitat distribution and improved mapping accuracy, allowing for a detailed analysis of the diversity, species composition, and structure of seagrass communities in the research area. This is the scientific foundation for resource management, marine environment protection, and biodiversity conservation, particularly in the Da Lon Reef area and the Truong Sa Islands in general.

5. Conclusions

Da Lon Reef in the Truong Sa Islands, Vietnam, is a significant entity whose benefits are not affected by its location and role, particularly in the shallow sea ecosystem. Based on integrating the Pléiades high-resolution remote sensing image data with field survey results, a benthic habitat map was established in the Big Reef area with high accuracy for seven classes of benthic habitats. In addition, five seagrass species were identified at Da Lon Reef, and simultaneously, the structure of seagrass communities was determined, and the morphology of each species was described. The seagrass ecosystem in the Da Lon Reef area is highly diverse, with 5 species of recorded seagrass distributed in the lagoon area at depths ranging from 2 to 6 m. The area is less affected by wave dynamics than seagrass ecosystems in the wave zone, such as Nam Yet, Son Ca, and Phan Vinh Island in the Truong Sa Islands.

Our study integrated data obtained from Da Lon Reef, an essential entity in the Spratly Islands, with that from a logistics base to provide a reference for the development of policies and solutions for natural resource management, protection of the marine and island environment, and conservation of Da Lon Reef biodiversity in particular and the Truong Sa Islands, Vietnam, in general.

In the future, image resolution will be increasingly improved following the development of remote sensing technology and UAVs, thus enhancing map accuracy. In addition, surveys and verifications to assess map accuracy are essential to establishing land cover maps and distribution maps of biomes based on remote sensing image materials.

Acknowledgments

This study was supported by project KCB-TS03: "Studying the marine - island landscapes of Truong Sa Islands for management and sustainable use of resources based on the application of remote sensing technology and GIS." The authors thank the Joint Vietnam-Russia Tropical Science and Technology Research Center for providing the authors the opportunity to participate in field trips to collect data in Truong Sa.

References

Al Hadi A., Wicaksono P., 2021. Accuracy assessment of relative and absolute water column correction methods for benthic habitat mapping in Parang Island. IOP Conference Series: Earth and Environmental Science, 686, 012034. https://doi.org/10.1088/1755-1315/686/1/012034.

Alberotanza L., et al., 2003. Satellite remote sensing for seagrass mapping in the Venice lagoon. Conference: 37th CIESM congress, Barcelona (Spain).

Anggoro A, Siregar V, Agus SB., 2015. Geomorphic zones mapping of coral reef ecosystem with obia method, case study in pari island. J Remote sens and Digital Image Processing, 12(1).

Barrell J., Grant J., Hanson A., Mahoney M., 2015. Evaluating the complementarity of acoustic and satellite remote sensing for seagrass landscape mapping. International Journal of Remote Sensing, 36, 1-26. https://doi.org/10.1080/01431161.2015.1076208.

Butler J., Purkis L., Purkis S., Yousif R., Al-Shaikh I., 2021. A benthic habitat sensitivity analysis of Qatar's coastal zone. Marine Pollution Bulletin, 167, 112333. https://doi.org/10.1016/j.marpolbul.2021.112333.

Butler J., Purkis S., Yousif R., Al-Shaikh I., Warren C., 2020. A high-resolution remotely sensed benthic habitat map of the Qatari coastal zone. Marine Pollution Bulletin, 160. https://doi.org/10.1016/j.marpolbul.2020.111634.

Congalton R.G., Green K., 20199. Assessing the accuracy of remotely sensed data: Principles and practices, Third Edition. CRC Press, 348. https://doi.org/10.1201/9780429052729.

Dang H., Trung D., Kuznetsov A.N., Phuong V., 2022. Classification and mapping of marine-island landscape in Nam Yet Island, Truong Sa Islands, Vietnam. Vietnam Journal of Earth Sciences, 1-21. https://doi.org/10.15625/2615-9783/17178.

Dang Hoi N., Trung Dung N., Viet Dung V., Quan V.V.D., 2022. Establishing distribution maps and structural analysis of seagrass communities based on high-resolution remote sensing images and field surveys: a case study at Nam Yet Island, Truong Sa Archipelago, Vietnam. Landscape and Ecological Engineering, 18, 405-419. https://doi.org/10.1007/s11355-022-00502-0.

Dekker A., Brando V., Anstee J., Fyfe S., Malthus T., Karpouzli E., 2006. Remote sensing of seagrass ecosystems: use of spaceborne and airborne sensors. In: LARKUM, A.W.D., ORTH, R.J., DUARTE, C.M. (Eds.), Seagrasses: Biology, Ecology and Conservation. Springer Netherlands, Dordrecht, 347-359. https://doi.org/10.1007/978-1-4020-2983-7_15.

Dekker A., Mount R., Jordan A., 2007. Satellite and airborne imagery including aerial photography for benthic habitat mapping. Special Paper - Geological Association of Canada, 11-27.

El Shaffai A., 2011. Field Guide to Seagrasses of the Red Sea (First Edition). Gland, Switzerland: IUCN and Courbevoie, 55p.

English S., Wilkinson C., Baker V., 1997. Survey Manual for Tropical Marine Resources. 2nd edition. Australian Institute of Marine Science, 148p.

Fauzan M.A., 2016. The use of Sentinel-2 MSI data in small island's nearshore benthic habitat mapping. Prepared for HISAS 14, Innovation and Technology. https://doi.org/ 10.31230/osf.io/nrup7.

Fernandez V., Martimort P., Spoto F., Sy O., Laberinti P., 2013. Overview Of Sentinel-2. Proc SPIE. Doi: 10.1117/12.2028755.

Fourqurean J., Durako M., Hall M., Hefty L., 2001. Seagrass distribution in South Florida. In: The everglades, florida bay, and coral reefs of the florida keys, 522p. https://doi.org/10.1201/9781420039412-22.

Ginting D., Purwanto A., 2021. Semi-Automatic Classification Model on Benthic Habitat Using Spot-7 Imagery in Penerusan Bay, Bali. Jurnal Segara, 17, 185. https://doi.org/10.15578/segara.v17i3.9771.

Grech A., et al., 2012. A comparison of threats, vulnerabilities and management approaches in global seagrass bioregions. Environmental Research Letters 7(2), 1-8. https://doi.org/10.1088/1748-9326/7/2/024006.

Hafeez S., Wong M.S., Abbas S., Kwok C.Y., Nichol J., Ho Lee K., Tang D., Pun L., 2019. Detection and Monitoring of Marine Pollution Using Remote Sensing Technologies. In Monitoring of Marine Pollution; Fouzia, H.B., Ed.; IntechOpen: London, UK. Chapter, 2, 26.

Hafizt M., Iswari M., Prayudha B., 2017. Assessment of Landsat-8 Classification Method for Benthic Habitat Mapping in Padaido Islands, Papua. Oseanologi Dan Limnologi Di Indonesia, 2, 1-13.

Hancox D.J., Prescott J.R.V., Schofield C.H., 1995. A Geographical Description of the Spratly Islands and an Account of Hydrographic Surveys Amongst Those Islands: International Boundaries Research Unit, University of Durham, 88p. ISBN 1-897643-18-7.

Harris P., Baker E., 2012. Why Map Benthic Habitats?. Seafloor Geomorphology as Benthic Habitat, 3-22. https://doi.org/10.1016/B978-0-12-385140-6.00001-3.

Hartog C., 1970. The seagrasses of the world. Verhandlingen Koninglijk Nederlandse Akademie Wetenschapen Afdeling Natuurkunde, 59, 1-275.

Hassan H., Nadaoka K., Nakamura T., 2020. Semiautomated Mapping of Benthic Habitats and Seagrass Species Using a Convolutional Neural Network Framework in Shallow Water Environments. Remote Sensing, 12, 4002. https://doi.org/10.3390/rs12234002.

Hedley J., Russell B., Randolph K., Dierssen H., 2016. A physics-based method for the remote sensing of seagrasses. Remote Sensing of Environment, 174, 134-147. https://doi.org/10.1016/j.rse.2015.12.001.

Janowski Ł., Wróblewski R., Dworniczak J., Kolakowski M., Rogowska K., Wojcik M., Gajewski J., 2021. Offshore benthic habitat mapping based on object-based image analysis and geomorphometric approach. A case study from the Slupsk Bank, Southern Baltic Sea. Science of The Total Environment, 801, 149712. https://doi.org/10.1016/j.scitotenv.2021.149712.

Kabiri K., Rezai H., Moradi M., 2020. A drone-based method for mapping the coral reefs in the shallow coastal waters - case study: Kish Island, Persian Gulf. Earth Science Informatics, 13. https://doi.org/10.1007/s12145-020-00507-z.

Kendall M., Costa B., McKagan S., Johnston L., Okano D., 2017. Benthic Habitat Maps of Saipan Lagoon. NOAA Technical Memorandum NOS NCCOS 229. Silver Spring, MD., 77p.

Kennedy E., Roelfsema C., Lyons M., Kovacs E., Borrego Acevedo R., Roe M., Phinn S.R., Larsen K., Murray N.J., Yuwono D., Wolff J., Tudman P., 2021. Reef Cover, a coral reef classification for global habitat mapping from remote sensing. Scientific Data, 8, 196. https://doi.org/10.1038/s41597-021-00958-z.

Khairunnisa K., Setyobudiandi I., Boer M., 2021. Seagrass distribution in the east coast of Bintan. IOP Conference Series: Earth and Environmental Science, 782, 042001. https://doi.org/10.1088/1755-1315/782/4/042001.

Khaled M., Ahmed M., Kafrawy S., 2020. Benthic habitat mapping using remote sensing data at Hurghada region, Red Sea coast, Egypt. Assiut University Journal of Multidisciplinary Scientific Research, 20-34.

Kirkman H., 1996. Baseline and Monitoring Methods for Seagrass Meadows. Journal of Environmental Management, 47, 191-201. https://doi.org/10.1006/jema.1996.0045.

Lamit N., Tanaka Y., Mohamed H., 2017. Seagrass diversity in Brunei Darussalam: first records of three

species. Scientia Bruneiana, 16, 48-52. https://doi.org/10.46537/scibru.v16i2.65.

Luong C., Manh Nguyen L., Hung V., Tien D., Tran Dinh L., 2020. The status of seagrass communities in some islands of the Spratly Islands. Journal of Marine Science and Technology, 20(3), 285-295. https://doi.org/10.15625/1859-3097/20/3/15076.

Mascarenhas V., Keck T., 2018. Marine Optics and Ocean Color Remote Sensing, In YOUMARES 8-Oceans Across Boundaries: Learning from Each Other; Springer: Cham, Switzerland, 41p.

Vlasova G.A., Demenok M.N., Hoan P.S., Dung N.T.T., Tuan N.V., Thinh N.D., Trung P.B., Binh T.V., 2020. Distribution features of meteorological parameters in Truong Sa archipelago area. Vietnam Journal of Marine Science and Technology, 20(4), 405-416. https://doi.org/10.15625/1859-3097/15323.

McGrath R., 2010. Kappa Coefficient. in: The Corsini Encyclopedia of Psychology. https://doi.org/10.1002/9780470479216.corpsy0484.

Mellors J., Marsh H., Carruthers T., Waycott M., 2002. Testing the sediment-trapping paradigm of seagrass: Do seagrasses influence nutrient status and sediment structure in tropical intertidal environments? Bulletin of Marine Science, 71(3).

Nababan B., Mastu L.O., Idris N., Panjaitan J., 2021. Shallow-Water Benthic Habitat Mapping Using Drone with Object Based Image Analyses. Remote Sensing, 13, 4452. https://doi.org/10.3390/rs13214452.

Navulur K., 2006. Multispectral Image Analysis Using the Object-Oriented Paradigm. 1st Edition. Boca Raton, 204p. https://doi.org/10.1201/9781420043075.

Phillips R.C., Menez E.G., 1988. Seagrasses, Smithsonian Contributions to the Marine Sciences, 34, 1-104. https://doi.org/10.5479/si.01960768.34.

Porskamp P., Rattray A., Young M., 2018. Multiscale and Hierarchical Classification for Benthic Habitat Mapping. Geosciences, 8, 119. https://doi.org/10.3390/geosciences8040119.

Roy D., Wulder M., Loveland T., Woodcock C., Allen R., Anderson M., Helder D., Irons J.R., Johnson D.M., Kennedy R., Scambos T.A., Schaaf C.B., Schott J.R., Sheng Y., Vermote E.F., Belward A.S., Bindschadler R., Cohen W.B., Gao F., Hipple J.D., Hostert P., Huntington J., Justice C.O., Kilic A., Kovalskyy V., Lee Z.P., Lymburner L., Masek J.G., McCorkel J., Shuai Y., Trezza R., Vogelmann J., Wynne R.H., Zhu Z., 2014. Landsat-8: Science and Product Vision for Terrestrial Global Change Research. Remote Sensing of Environment, 145, 154-172. https://doi.org/10.1016/j.rse.2014.02.001

Ruiz Fernandez J.M., Boudouresque C., Enríquez S., 2009. Seagrass ecosystems and Mediterranean seagrasses. Botanica Marina, 52, 369-381. https://doi.org/10.1515/BOT.2009.058.

Short F., Coles R., 2002. Global Seagrass Research Methods. Aquaculture, 212(1). https://doi.org/10.1016/S0044-8486(02)00307-1.

Short F., Short C., Novak A., 2016. In: Finlayson, C.M., Milton, G.R., Prentice, R.C., Davidson, N.C. (Eds.), Seagrasses. In The Wetland Book II: Distribution, description and conservation. Springer Science: Dordrecht, The Netherlands. https://doi.org/10.1007/978-94-007-6173-5_262-1.

Short F.T., McKenzie L.J., Coles R.G., Vidler K.P., 2002. Manual for Scientific Monitoring of Seagrass Habitat SeagrassNet. QDPI, QFS, Cairns, 56.

Sinaga S., Yulianto A., Putri K., Bayudin, Wicaksono P., 2016. The Use of Worldview-2 Imagery for Benthic Habitat Mapping at Bangsring, Banyuwangi Regency. 2nd International Conference of Indonesian Society for Remote SensingAffiliation: Remote Sensing, Faculty of Geography, University of Gadjah Mada, PUSPICS. https://doi.org/10.13140/RG.2.2.10006.68168.

Smith T., Mittermayr A., Legare B., Fox S., Borrelli M., 2019. Benthic Habitat Mapping in Wellfleet Harbor and Vicinity. 19-CL08. Center for Coastal Studies, 74p. https://doi.org/10.13140/RG.2.2.28258.35526.

Taha L., Elsayed R., 2021. Assessment of Approaches for the Extraction of Building Footprints from Pléiades Images. Geomatics and Environmental Engineering, 15(4), 101-116. https://doi.org/10.7494/geom.2021.15.4.101.

Tamondong A., Blanco A., Fortes M., Nadaoka K., 2013. Mapping of seagrass and other benthic habitats in Bolinao, Pangasinan using Worldview-2 satellite image. IGARSS 2013-2013

IEEE International Geoscience and Remote Sensing Symposium, p.1579. https://doi.org/10.1109/IGARSS.2013.6723091.

Tran Van D., 2008. Mapping benthic habitats in Con Son Bay, Vietnam from IKONOS satellite image. The 9th Pan Ocean Remote Sensing Conference, 2-6 December 2008, Guangzhou, ChinaAt: Guangzhou, China.

Velez-Reyes M., Goodman J., Castrodad-Carrau A., Jiménez-Rodriguez L., Hunt S., Armstrong R., 2006. Benthic habitat mapping using hyperspectral remote sensing, Proceedings of SPIE: Remote Sensing of the Ocean, Sea Ice, and Large Water Regions, 6360.

Wahidin N., Siregar V., Nababan B., Jaya I., Wouthuyzen S., 2015. Object-based Image Analysis for Coral Reef Benthic Habitat Mapping with Several Classification Algorithms. Procedia Environmental Sciences, 24, 222-227. https://doi.org/10.1016/j.proenv.2015.03.029.

Wicaksono P., 2014. The use of image rotations on multispectral- based benthic habitats mapping. The 12th Biennial Conference of PORSEC 2014. Denpasar, Bali: PORSEC.

Wicaksono P., Adhimah F., 2017. Accuracy assessments of pan-sharpened image for benthic habitats mapping. Geoplanning: Journal of Geomatics and Planning, 4, 27. https://doi.org/10.14710/geoplanning.4.1.27-40.

Wicaksono P., Aryaguna P., Lazuardi W., 2019. Benthic Habitat Mapping Model and Cross Validation Using Machine-Learning Classification Algorithms. Remote Sensing, 11, 1279. https://doi.org/10.3390/rs11111279.

Wicaksono P., Fauzan M.A., Asta S., 2019. Assessment of Sentinel-2A multispectral image for benthic habitat mapping. IET Image Processing, 14. https://doi.org/10.1049/iet-ipr.2018.6044.

Wicaksono P., Kumara W., Fauzan M.A., Noviaris R., Lazuardi W., 2020. Sentinel-2A and Landsat 8 OLI to model benthic habitat biodiversity index. Geocarto International, 1-13. https://doi.org/10.1080/10106049.2020.1790673.

Yoder M., Tandingan De Ley I., King I.W., Mundo-Ocampo M., Mann J., Blaxter M., Potras L., De Ley P., 2006. DESS: a versatile solution for preserving morphology and extractable DNA of nematodes. Nematology, 8(3), 367-376. http://dx.doi.org/10.1163/156854106778493448.